

See discussions, stats, and author profiles for this publication at: <https://www.researchgate.net/publication/10783383>

# The structure and stability of Si 60 and Ge 60 cages: A computational study

ARTICLE *in* JOURNAL OF COMPUTATIONAL CHEMISTRY · JUNE 2003

Impact Factor: 3.59 · DOI: 10.1002/jcc.10266 · Source: PubMed

CITATIONS

27

READS

60

8 AUTHORS, INCLUDING:



Zhongfang Chen

University of Puerto Rico at Rio Piedras

221 PUBLICATIONS 8,028 CITATIONS

SEE PROFILE



Gotthard Seifert

Technische Universität Dresden

428 PUBLICATIONS 14,304 CITATIONS

SEE PROFILE



Anselm H. C. Horn

Friedrich-Alexander-University of Erlangen-Nü...

66 PUBLICATIONS 1,264 CITATIONS

SEE PROFILE

# The Structure and Stability of Si<sub>60</sub> and Ge<sub>60</sub> Cages: A Computational Study

ZHONGFANG CHEN,<sup>1,2</sup> HAIJUN JIAO,<sup>3,4</sup> GOTTHARD SEIFERT,<sup>5</sup> ANSELM H. C. HORN,<sup>6</sup>  
DENGKE YU,<sup>7</sup> TIM CLARK,<sup>6</sup> WALTER THIEL,<sup>8</sup> PAUL VON RAGUÉ SCHLEYER<sup>1,2</sup>

<sup>1</sup>Institut für Organische Chemie, Universität Erlangen-Nürnberg, Henkestraße 42,  
91054 Erlangen, Germany

<sup>2</sup>Computational Chemistry Annex, The University of Georgia, Athens, Georgia 30602-2525

<sup>3</sup>Department of Chemistry, Shanxi Normal University, Linfen, People's Republic of China

<sup>4</sup>Leibniz-Institut an der Universität Rostock e. V., Buchbinderstraße 5-6, 18055 Rostock, Germany

<sup>5</sup>Institut für Physikalische Chemie und Elektrochemie, Technische Universität Dresden,  
Mommensenstraße 13, D-01062 Dresden, Germany

<sup>6</sup>Computer Chemie Centrum, Universität Erlangen-Nürnberg, Nügelsbachstraße 25,  
D-91052 Erlangen, Germany

<sup>7</sup>Fritz-Haber-Institut der Max-Planck-Gesellschaft, Faradayweg 4-6,  
D-14195 Berlin-Dahlem, Germany

<sup>8</sup>Max-Planck-Institut für Kohlenforschung, Kaiser-Wilhelm-Platz 1,  
45470 Mülheim an der Ruhr, Germany

Received 25 September 2002; Accepted 20 December 2002

**Abstract:** Structural studies of fullerene-like Si<sub>60</sub> and Ge<sub>60</sub> cages using *ab initio* methods were augmented by density functional tight-binding molecular dynamics (DFTB-MD) simulations of finite temperature effects. Neither the perfect *I<sub>h</sub>* symmetry nor the distorted *T<sub>h</sub>* structures are true minima. The energies of both are high relative to distorted, lower symmetry minima, *C<sub>i</sub>* and *T*, respectively, which still preserve *C<sub>60</sub>*-type connectivity. Both Si<sub>60</sub> and Ge<sub>60</sub> favor *C<sub>i</sub>* symmetry cages in which Si and Ge vertexes exhibit either near-trigonal or pyramidal geometries. These structural variations imply significant reactivity differences between different positions. The small magnetic shielding effects (NICS) indicate that aromaticity is not important in these systems. The inorganic fullerene cages have lower stabilities compared with their carbon analogs. Si<sub>60</sub> is stable towards spontaneous disintegration up to 700 K according to DFTB-MD simulations, and thus has potential for experimental observation. In contrast, Ge<sub>60</sub> preserves its cage structure only up to 200 K.

© 2003 Wiley Periodicals, Inc. J Comput Chem 24: 948–953, 2003

**Key words:** inorganic fullerenes; Si<sub>60</sub>; Ge<sub>60</sub>; DFT; DFTB

## Introduction

Soon after the discovery of fullerene, the structures of its silicon and germanium analogs were proposed and investigated at various level of theory. However, the literature does not agree, and the lowest energy geometries were not established. Most of the studies simply assumed Si<sub>60</sub> and Ge<sub>60</sub> to preserve the perfect *I<sub>h</sub>* symmetry cage structure of C<sub>60</sub> as the ground state.<sup>1</sup> Such intuitive geometries also were employed to model endohedral complexes<sup>2</sup> and double-layered heterofullerenes C<sub>60</sub>@Si<sub>60</sub>.<sup>1,3</sup> Even after taking other structures into account, Nagase et al.<sup>4</sup> found the hollow spherical cage still to be preferred energetically. However, several authors pointed out that icosahedral Si<sub>60</sub> is not stable and relaxes

into a distorted structure.<sup>5</sup> Tight-binding molecular dynamics simulations gave a puckered ball-like geometry (Khan and Broughton<sup>5a</sup>) and lower symmetry *C<sub>2h</sub>* structure (Menon and

**Correspondence to:** Z. Chen; e-mail: zhongfang.chen@organik.uni-erlangen.de

Contract/grant sponsor: Alexander von Humboldt Stiftung (Z. Chen, D. Yu)

Contract/grant sponsor: National Science Foundation; contract/grant number: CHE-0209857

This article includes Supplementary Material available from the authors upon request or via the Internet at <ftp://ftp.wiley.com/public/journals/jcc/suppmat/24/948> or <http://www.interscience.wiley.com/jpages/0192-8651/suppmat/v24.948.html>

**Table 1.** Calculated Relative Energies (kcal/mol), HOMO-LUMO Gap Energies (eV), the Number of Imaginary Frequencies (NImag), and Lowest Vibrational (Real or Imaginary) Frequencies ( $\omega_1$ ; cm<sup>-1</sup>) for Si<sub>60</sub>.

Symmetry	$I_h$	$T_h$	$T$	$C_i$
$E_{\text{rel}}^a$	76.5	72.5	3.6	0.0
NImag <sup>a</sup>	16	10	0	0 <sup>c</sup>
$\omega_1^a$	-211.3	-164.7	67.5	62.9 <sup>c</sup>
$E_{\text{gap}}^a$	4.41	4.14	4.54	4.68
$E_{\text{rel}}^b$	91.3	56.2	4.7	0.0
$E_{\text{gap}}^b$	1.31	1.06	1.31	1.40
$E_{\text{rel}}^d$	132.8	66.4	4.2	0.0

<sup>a</sup>At HF/3-21G.<sup>b</sup>At B3LYP/6-31G\*.<sup>c</sup>At HF/STO-3G.<sup>d</sup>At DF-TB.

Subbaswamy).<sup>5b</sup> According to full-potential LMTO molecular dynamics (FP-LMTO-MD),<sup>5c,5d</sup> the icosahedral Si<sub>60</sub> and Ge<sub>60</sub> cages distort to  $T_h$  symmetry. First-principle quantum-molecular-dynamics calculations predict the fullerene-like structure to be metastable, but still relatively low in energy, while the compact network (high coordination) structure is the equilibrium configuration.<sup>5e</sup> Based on tight-binding molecular dynamic calculations using the bulk diamond lattice fragments as the initial structure, Yu et al. proposed that the most stable Si<sub>60</sub> form is composed of cage subunits like Si<sub>6</sub>, Si<sub>7</sub>, Si<sub>10</sub> and Si<sub>12</sub>.<sup>5f</sup>

A similarly confusing picture exists experimentally. The fullerene structure was implied by a saturation study of Si<sub>60</sub> positive ions, which revealed that ammonia only binds to a small number of cluster sites<sup>6</sup> (as for C<sub>60</sub>).<sup>7</sup> A stacked naphthalene-like layer structure was suggested by the fragmentation analysis of Si<sub>60</sub> positive ions.<sup>8</sup>

Less attention has been paid to germanium than to silicon fullerenes. The perfect  $I_h$  symmetry Ge<sub>60</sub> cage structure has been proposed by Nagase<sup>1d</sup> and by Leszczynski.<sup>1k</sup> However, Slanina found the Ge<sub>60</sub> cage to be distorted while retaining the fullerenic connectivity; in contrast, he claimed Si<sub>60</sub> still to exhibit the exact  $I_h$  symmetry.<sup>1g</sup> Menon declared that among the group IV elements, perfect icosahedral symmetry is unique to carbon.<sup>5b</sup> Ge<sub>60</sub> has been found to favor a distorted cage structure with  $T_h$  symmetry by full-potential molecular dynamic studies.<sup>5c</sup>

To clarify the bewildering discrepancies in the literature and to gain further insight into the electronic properties of Si<sub>60</sub> and Ge<sub>60</sub> cages, we have now optimized structures with different symmetries and performed vibrational frequency analyses at *ab initio* and DFT levels. Density functional tight-binding molecular dynamics (DFTB-MD) simulations revealed the finite temperature effects on the stabilities.

## Computational Details

The geometries were fully optimized and vibrational frequencies were computed at the Hartree-Fock (HF) level with the 3-21G

basis set for silicon and the Lan12DZ pseudopotential for germanium (except for  $C_i$  symmetry Si<sub>60</sub> where the STO-3G basis set was used for frequency analysis).  $I_h$  and  $T_h$  symmetry structures were computed initially; following the displacements of the first of the imaginary frequencies which resulted then led to the  $C_i$  and  $T$  symmetry cages. Further full optimizations were performed using the B3LYP hybrid density functional method<sup>9</sup> with 6-31G\* and Lan12DZ basis sets for silicon and germanium, respectively. Moreover, single-point energy computations were carried out for Ge<sub>60</sub> using the Lan2DZp basis set (with one additional set of d polarization functions at Ge).<sup>10</sup> Nucleus-independent chemical shifts (NICS),<sup>11</sup> calculated at the centers of the cages and of the individual rings, evaluated the aromaticity. All these calculations employed the GAUSSIAN 98 suite of programs.<sup>12</sup> The relative total energies at both HF and DFT levels, the number of imaginary frequencies (NImag), and the lowest-magnitude (imaginary) vibrational frequencies at the HF level are summarized in Tables 1 and 2. To investigate the finite temperature effects, molecular dynamics (MD) simulations were performed using the Density-Functional Tight-Binding (DFTB) method;<sup>13</sup> a time step of 0.24 fs was chosen in the total simulation time of 12 ps.

## Results and Discussion

Although silicon and carbon are isovalent group IV elements, it is well known that they have different chemical bonding properties.<sup>14</sup> Due to the versatile bonding behavior and the ability to form single, double, and triple bonds, carbon can form many diverse structures such as graphite, diamond, fullerenes, carbon nanotubes, amorphous carbon, porous carbon, and graphite intercalation compounds. Carbon clusters can utilize strong  $\pi$ -bonds to produce chains, rings, cages, and tubes. In contrast, silicon does not form energetically favorable double and triple bonds, also in cages. This is indicated by various distorted<sup>5d,15</sup> silicon clusters that also may

**Table 2.** Calculated Relative Energies (kcal/mol), HOMO-LUMO Gap Energies (eV), the Number of Imaginary Frequencies (NImag), and Lowest Vibrational (Real or Imaginary) Frequencies ( $\omega_1$ ; cm<sup>-1</sup>) for Ge<sub>60</sub>.

Symmetry	$I_h$	$T_h$	$T$	$C_i$
$E_{\text{rel}}^a$	163.7	123.7	3.5	0.0
NImag <sup>a</sup>	19	13	0	0
$\omega_1^a$	-145.9	-60.6	33.6	35.2
$E_{\text{gap}}^a$	4.45	3.90	4.46	4.55
$E_{\text{rel}}^b$	206.4	86.8	4.8	0.0
$E_{\text{gap}}^b$	0.99	1.02	1.28	1.40
$E_{\text{rel}}^c$	212.8	91.2	6.4	0.0
$E_{\text{rel}}^d$	275.3	80.3	15.2	0.0

<sup>a</sup>At HF/LANL2DZ.<sup>b</sup>At B3LYP/LANL2DZ.<sup>c</sup>At B3LYP/LANL2DZp//B3LYP/LANL2DZ.<sup>d</sup>At DF-TB. The validity of DFTB for describing germanium containing systems has been shown in Hajnal, Z.; Vogg, G.; Meyer, L. J. P.; Szuëcs, B.; Brandt, M. S.; Frauenheim, T. Phys Rev B 2001, 64, 33311.

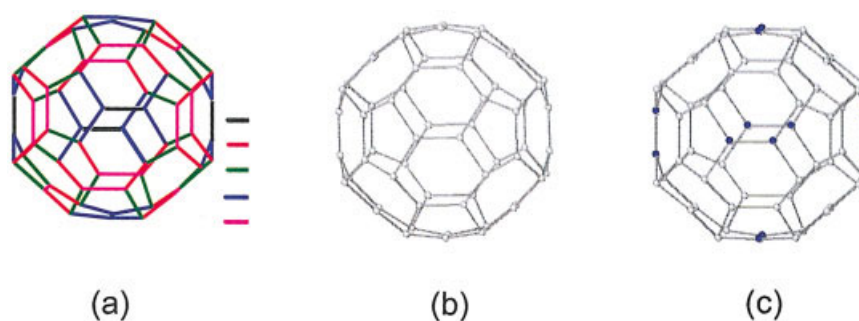


**Figure 1.** DFT optimized  $T_h$  symmetry clusters (a) five types of bonds (given in Table 3); (b)  $\text{Si}_{60}$ ; (c)  $\text{Ge}_{60}$ ; the germanium atoms with  $\pi$  conjugation are distinguished by blue coloring.

utilize hypercoordinate bonding.<sup>16</sup> Similarities between germanium and silicon clusters have been reported,<sup>5c,17</sup> and are supported experimentally by photofragmentation and reactivity results.<sup>18</sup>

Data in Tables 1 and 2 confirm that  $I_h$  symmetry  $\text{Si}_{60}$  and  $\text{Ge}_{60}$  clusters are far from being true minima. Frequency analyses at the HF level of theory reveal 16 and 19 imaginary frequencies, respectively! The vectors of the first imaginary frequencies lead to  $C_i$  symmetry clusters that are true minima both for  $\text{Si}_{60}$  and  $\text{Ge}_{60}$ .

Employing full-potential LMTO molecular dynamics (FP-LMTO-MD) method,<sup>5c,5d</sup> Li et al. found that  $\text{Si}_{60}$  and  $\text{Ge}_{60}$  distort to  $T_h$  symmetry. However, our frequency analyses indicate that  $T_h$  symmetry structures are also higher order saddle points with 10 and 13 imaginary frequencies, respectively (Tables 1 and 2). Instead, lower energy  $T$  symmetry minima were obtained following the first imaginary vibration in  $T_h$  structures for both  $\text{Si}_{60}$  and  $\text{Ge}_{60}$ .

In  $I_h$  symmetrical clusters, all atoms have near trigonal geometries. The bond lengths for 6-6 and 6-5 bonds are 2.236 and 2.284 Å in  $\text{Si}_{60}$  and 2.363 and 2.426 Å in  $\text{Ge}_{60}$ , respectively. The previously proposed  $T_h$  symmetry clusters have five types of bonds (shown in Fig. 1; bond lengths are given in Table 3). These structures resemble puckered balls with some pyramidally distorted vertexes.

At our DFT level, the  $C_i$  minima are preferred over the  $T$  minima by 4.7 and 4.8 kcal/mol for  $\text{Si}_{60}$  and  $\text{Ge}_{60}$ , respectively (adding polarization functions does not change the  $\text{Ge}_{60}$  isomer energy order, Table 2). The optimized  $T$  symmetry geometries are shown in Figure 2 their bond lengths are summarized in Table 4.

**Table 3.** Optimized Bond Lengths (Å) of  $\text{Si}_{60}$  ( $T_h$ ) and  $\text{Ge}_{60}$  ( $T_h$ ).<sup>a,b</sup>

Bond	$\text{Si}_{60}$	$\text{Ge}_{60}$
<i>a</i>	2.226	2.367
<i>b</i>	2.274	2.469
<i>c</i>	2.302	2.501
<i>d</i>	2.320	2.514
<i>e</i>	2.287	2.460

<sup>a</sup>See Figure 1.

<sup>b</sup>B3LYP/6-31G\* for  $\text{Si}_{60}$ , B3LYP/LANL2DZ for  $\text{Ge}_{60}$ .

Eight sets of bonds exist in  $T$  symmetry clusters; the ranges are 2.224–2.337 Å in  $\text{Si}_{60}$  and 2.375–2.551 Å in  $\text{Ge}_{60}$ . Figure 3 shows the optimized structures of the most stable  $C_i$  clusters, the bond length ranges are 2.234–2.344 Å in  $\text{Si}_{60}$  and 2.393–2.561 Å in  $\text{Ge}_{60}$ . Some atoms have three nearly coplanar neighbors (24 in  $T$  and 30 in  $C_i$ ), while others favor tetrahedral-like geometries, with atoms popped outside the plane of their neighbors. These atoms should be more reactive than their trigonal counterparts. The DFT binding energies of the most stable  $\text{Si}_{60}$  and  $\text{Ge}_{60}$  clusters are only 3.36 and 2.69 eV/atom, about or less than half of the binding energy of  $\text{C}_{60}$  (6.98 eV/atom), which indicates their relative low stability compared to their carbon analog. To assist future experiments, the vertical ionization potentials (IP, 6.234 and 6.166 eV) and electron affinities (EA, 3.141 and 3.360 eV) of the most stable  $C_i$  symmetrical  $\text{Si}_{60}$  and  $\text{Ge}_{60}$  cages, respectively, also were computed.

Further insight into the bonding nature of silicon and germanium fullerenes was provided by NBO (Natural Bonding Orbital) analyses<sup>19</sup> at the B3LYP level. Regardless of different symmetries ranging from  $I_h$  to  $C_i$ , there are 120 BD (two-center bond) NBOs in  $\text{Si}_{60}$ , 90 corresponding to  $\sigma$  bonds and 30 to  $\pi$  bonds, with nearly pure  $p$  character at the silicon atoms. Hence, there are 30 double bonds at the hexagon-hexagon junctions of  $\text{Si}_{60}$ , which resembles  $\text{C}_{60}$  in  $I_h$  symmetry. However, unlike the nonpolarized bonds in  $\text{C}_{60}$ , the  $\pi$  bonds in the most stable  $C_i$  symmetry  $\text{Si}_{60}$  cage are heavily polarized with ca. 66% towards the pyramidal Si atoms, whereas the  $\sigma$  bonds are only slightly polarized. The  $\pi$  conjugation around the whole silicon cage shortens the silicon-silicon bond lengths significantly; the double bond range is 2.234–2.301 Å, somewhat shorter than the Si-Si bond length in bulk silicon (2.35 Å).

However,  $\text{Ge}_{60}$  is different. The unrealistic  $\text{Ge}_{60}$  ( $I_h$ ) has bonding similar to  $\text{C}_{60}$ , with 30 nonpolarized single bonds and 30 nonpolarized double bonds. But the distorted  $\text{Ge}_{60}$  cages only have six  $\pi$  bonds located at the hexagon-hexagon junctions (Figs. 1–3) and 90  $\sigma$  bonds, instead of the other 24  $\pi$  bonds, there are 24 lone pair NBOs. The  $\pi$  bonds still have >90%  $p$  character and while the  $\pi$  bonds are nonpolarized in  $T_h$  and  $T$  symmetrical cages, some polarization towards the trigonal atoms (ca. 56%) exists in  $\text{Ge}_{60}$  ( $C_i$ ). The double bond lengths are nearly the same, 2.367, 2.375, and 2.393 Å in the  $T_h$ ,  $T$ , and  $C_i$  symmetry cages, respectively,

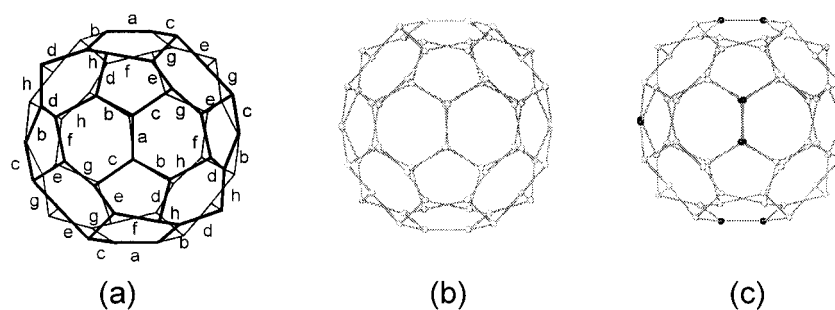


**Figure 2.** DFT optimized  $T$  symmetrical clusters (a) eight types of bonds (given in Table 4); (b)  $\text{Si}_{60}$ ; (c)  $\text{Ge}_{60}$ ; the germanium atoms with  $\pi$  conjugation are distinguished by dark coloring.

shorter than the single bond in bulk germanium (2.45 Å). The 24 lone pairs in the distorted  $\text{Ge}_{60}$  cages are located at the pyramidal atoms at other hexagon–hexagon junctions without  $\pi$  conjugation. Except for the six double bonds mentioned above, all the other 84 bonds, at both hexagon–hexagon and hexagon–pentagon junctions are single bonds in the distorted cages, even longer than the single bond in the bulk. Figure 4 shows the  $\pi$  bonds in  $\text{Si}_{60}$  ( $C_i$ ) and the lone pair electrons in  $\text{Ge}_{60}$  ( $C_i$ ) to illustrate the difference of the bonding properties in the most stable distorted cages.

As in the inorganic  $\text{Si}_{60}$  and  $\text{Ge}_{60}$  fullerenes, the inorganic benzene homologs,  $\text{Si}_6\text{H}_6$  and  $\text{Ge}_6\text{H}_6$ , also do not have planar energy minima. The most stable  $\text{Si}_6\text{H}_6$  and  $\text{Ge}_6\text{H}_6$  geometries have  $D_{3d}$  symmetry; the  $D_{6h}$  form has NImag = 1 for  $\text{Si}_6\text{H}_6$  and NImag = 3 for  $\text{Ge}_6\text{H}_6$ . The  $D_{3d}$  structures of  $\text{Si}_6\text{H}_6$  and  $\text{Ge}_6\text{H}_6$  are more stable than the  $D_{6h}$  forms by 2.3 and 14.5 kcal/mol at the B3LYP/6-311+G\*\* level. However, this distortion does not affect the aromaticity significantly, as indicated by their NICS(1) values of  $-12.8$  ( $D_{6h}$ ) and  $-11.4$  ( $D_{3d}$ ) ppm for  $\text{Si}_6\text{H}_6$ , as well as  $-14.5$  ( $D_{6h}$ ) and  $-9.9$  ( $D_{3d}$ ) ppm for  $\text{Ge}_6\text{H}_6$ ; these are comparable to the benzene NICS(1) of  $-10.7$  ppm.<sup>20</sup>

The modest aromaticity of  $\text{C}_{60}$ ,<sup>21</sup> is evidenced by the experimentally measured endohedral helium chemical shift ( $-6.3$  ppm),<sup>22</sup> which is close to the  $-8.0$  ppm computed NICS(0) value at the cage center (at GIAO-HF/3-21G//B3LYP/6-31G\*),<sup>23</sup> and the modest NICS(sum) =  $-34.3$  ppm of all the ring centers. How aromatic are the heavier  $\text{C}_{60}$  analogs,  $\text{Si}_{60}$  and  $\text{Ge}_{60}$ ? Table 5

summarizes computed NICS(0) and NICS(sum) values together with the relative energies of the four isomers. NICS(0) of the high energy  $I_h$  symmetry  $\text{Si}_{60}$  and  $\text{Ge}_{60}$  forms are both quite small (ca  $-1.5$  ppm), suggesting essentially nonaromatic character. Although the distorted but more stable isomers have somewhat more negative NICS(0) in the  $-6.0$  to  $-8.6$  ppm range, there is no apparent relationship with the relative energies. Strain and other effects are more important than aromatic stabilization energies. The NICS(sum) values are larger, but the variations do not correlate with the relative energies. In short, “aromaticity” is not the main effect responsible for the enhanced stability of the distorted  $\text{Si}_{60}$  and  $\text{Ge}_{60}$  cages.

The relative energy order given by DFT is reproduced well at the DFTB level by conjugate gradient relaxation calculations (see Tables 1 and 2). The latter method was also used to perform constant temperature molecular dynamics simulations to elucidate the stability of  $C_i$  symmetrical structures. During a simulation time of 12 ps (50,000 steps), heating  $\text{Si}_{60}$  ( $C_i$ ) to 700 K did not lead to structural breakdown and  $\text{Si}_{60}$  retained essentially the same structure, while the highest temperature of  $\text{Ge}_{60}$  to preserve its  $C_i$  symmetrical cage structure is only 200 K.  $\text{Si}_{60}$  and  $\text{Ge}_{60}$  collapse at 750 K and 250 K, respectively, in MD simulations of 12 ps. For comparison,  $\text{C}_{60}$  is stable against thermal disintegration up to 4500 K.<sup>24</sup> These MD simulations indicate that  $\text{Si}_{60}$  and  $\text{Ge}_{60}$  cages are less stable than their  $\text{C}_{60}$  analog, but  $\text{Si}_{60}$  should be viable, in contrast to  $\text{Ge}_{60}$ .

**Table 4.** Optimized Bond lengths (Å) of  $\text{Si}_{60}$  ( $T$ ) and  $\text{Ge}_{60}$  ( $T$ ).<sup>a,b</sup>

Bond	$\text{Si}_{60}$	$\text{Ge}_{60}$
<i>a</i>	2.224	2.375
<i>b</i>	2.290	2.457
<i>c</i>	2.334	2.535
<i>d</i>	2.311	2.519
<i>e</i>	2.325	2.529
<i>f</i>	2.337	2.551
<i>g</i>	2.299	2.502
<i>h</i>	2.293	2.494

<sup>a</sup>See Figure 2.

<sup>b</sup>B3LYP/6-31G\* for  $\text{Si}_{60}$ , B3LYP/LANL2DZ for  $\text{Ge}_{60}$ .

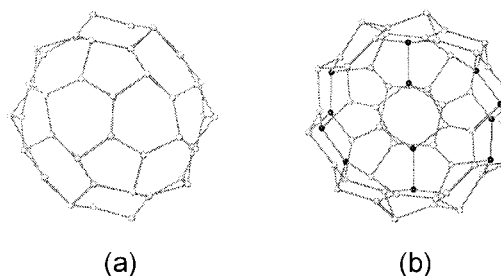


**Figure 3.** DFT optimized  $C_i$  symmetry clusters (a)  $\text{Si}_{60}$  (b)  $\text{Ge}_{60}$ ; the germanium atoms with  $\pi$  conjugation are distinguished by dark coloring.

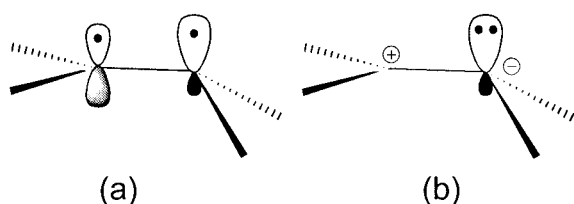


**Figure 4.** The  $\pi$  bonds in  $\text{Si}_{60}$  ( $C_i$ ) and lone pair electrons in  $\text{Ge}_{60}$  ( $C_i$ ).

## Conclusion

The lowest energy structures of  $\text{Si}_{60}$  and  $\text{Ge}_{60}$  cages, computed by *ab initio* and DFT methods, do not possess the perfect  $I_h$  symmetry of  $C_{60}$  nor the recently proposed distorted  $T_h$  structures. Both  $I_h$  and  $T_h$  forms are multiorder saddle points with unfavorable energies. Instead, the distorted  $C_i$  and  $T$  symmetrical cages (derived from  $I_h$  and  $T_h$  structures) are true minima, and preserve the  $C_{60}$  connectivity. The  $C_i$  symmetries are preferred energetically. Both near-trigonal and pyramidal vertexes are found in these  $C_i$  and  $T$  structures; this implies a significant reactivity difference between these two kinds of atoms. The geometries of  $\text{Ge}_{60}$  are rather similar to  $\text{Si}_{60}$ ; however, the nature of the bonding is quite different according to NBO analysis. Neither cage exhibits more than weak aromaticity, judging from the NICS values. The inorganic fullerene cages have lower thermal stabilities than their carbon analogue, but  $\text{Si}_{60}$  may be a viable preparative target.

## Acknowledgments

Z. Chen thanks Prof. Dr. Andreas Hirsch for helpful discussions and continuous supports, Prof. Dr. Matthias Scheffler for his hospitality in the Fritz-Haber-Institut, and B. X. Li (Zhejiang University, P. R. China) for providing the coordinates of  $\text{Si}_{60}$  ( $T_h$ ) obtained by FP-LMTO MD simulations.

**Table 5.** Relative Energies (kcal/mol) of  $\text{Si}_{60}$  and  $\text{Ge}_{60}$  Isomers, NICS(0) Values at the Cage Centers (ppm), and the NICS (sum) at All the Ring Centers.

	$I_h$	$T_h$	$T$	$C_i$
$\text{Si}_{60}$				
RE <sup>a</sup>	91.3	56.2	4.7	0.0
NICS(0) <sup>b</sup>	-1.4	-6.9	-6.0	-7.8
NICS(sum) <sup>b</sup>	-7.7	-65.8	-34.1	-56.7
$\text{Ge}_{60}$				
RE <sup>c</sup>	206.4	86.8	4.8	0.0
NICS(0) <sup>d</sup>	-1.5	-8.6	-6.5	-7.8
NICS(sum) <sup>d</sup>	3.5	-54.9	-4.3	-19.7

<sup>a</sup>B3LYP/6-31G\*.

<sup>b</sup>GIAO-HF/3-21G//B3LYP/6-31G\*.

<sup>c</sup>B3LYP/LanL2DZ.

<sup>d</sup>GIAO-HF/LanL2DZ//B3LYP/LanL2DZ.

## Supplementary Material Available

Total energies at HF, DFT, and DFTB levels, and Gaussian archive entries for DFT optimized structures are given.

## References

- (a) Nagase, S. *Polyhedron* 1991, 10, 1299; (b) Nagase, S.; Kobayashi, K. *Chem Phys Lett.* 1991, 187, 291; (c) Piqueras, M. C.; Crespo, R.; Orti, E.; Tomas, F. *Chem Phys Lett* 1993, 213, 509; (d) Nagase, S. *Pure Appl Chem* 1993, 65, 675; (e) Piqueras, M. C.; Crespo, R.; Orti, E.; Tomas, F. *Synth Met* 1993, 61, 155; (f) Piqueras, M. C.; Crespo, R.; Orti, E.; Tomas, F. *Chem Phys Lett* 1993, 213, 509; (g) Slanina, Z.; Lee, S. L. *Fullerene Sci Technol* 1994, 2, 459; (h) Zdetsis, A. D. *NATO ASI Ser, Ser B* 1996, 355, 455; (i) Crespo, R.; Piqueras, M. C.; Tomas, F. *Synth Met* 1996, 77, 13; (j) Turker, L. *Polycyclic Aromat Compd* 1999, 13, 119; (k) Leszczynski, J.; Yanov, I. *J Phys Chem A* 1999, 103, 396; (l) Gong, X. G.; Zheng, Q. Q. *Phys Rev B* 1995, 52, 4756.
- (a) de Proft, F.; Van Alsenoy, C.; Geerlings, P. *J Phys Chem* 1996, 100, 7440; (b) Turker, L. *ACH—Models Chem* 2000, 137, 511; (c) Turker, L. *J Mol Struct (Theochem)* 2001, 548, 185; (d) Turker, L. *J Mol Struct (Theochem)* 2001, 546, 45.
- (a) Osawa, S.; Harada, M.; Osawa, E.; Kiran, B.; Jemmis, E. D. *Fullerene Sci Technol* 1995, 3, 25; (b) Jemmis, E. D.; Leszczynski, J.; Osawa, E. *Fullerene Sci Technol* 1998, 6, 271.
- (a) Kobayashi, K.; Nagase, S. *Bull Chem Soc Jpn* 1993, 66, 3334; (b) Nagase, S.; Kobayashi, K. *Fullerene Sci Technol* 1993, 1, 299; (c) Slanina, Z.; Lee, S. L.; Kobayashi, K.; Nagase, S. *J Mol Struct (Theochem)* 1994, 118, 175.
- (a) Khan, F. S.; Broughton, J. Q. *Phys Rev B* 1991, 43, 11754; (b) Menon, M.; Subbaswamy, K. R. *Chem Phys Lett* 1994, 219, 219; (c) Li, B. X.; Jiang, M.; Cao, P. L. *J Phys Condens Matter* 1999, 11, 8517; (d) Li, B. X.; Cao, P. L.; Que, D. L. *Phys Rev B* 2000, 61, 1685; (e) Song, J.; Ulloa, S. E.; Drabold, D. A. *Phys Rev B* 1996, 53, 8042; (f) Yu, D. K.; Zhang, R. Q.; Lee, S. T. *Phys Rev B* 2002, 65, 245417.
- Jarrold, M. F.; Ijiri Y.; Ray, U. *J Chem Phys* 1991, 94, 3607.
- Hirsch, A.; Li, Q.; Wudl, F. *Angew Chem Int Ed Engl* 1991, 30, 1309.
- Jelski, D. A.; Wu, Z. C.; George, T. F. *J Cluster Sci* 1990, 1, 143.
- Becke, A. D. *J Chem Phys* 1993, 98, 5648.
- Huzinaga, S.; Andzelm, J.; Klobukowski, M.; Radzio-Andzelm, E.; Sakai Y.; Tatewaki, H. *Gaussian Basis Sets for Molecular Calculations*; Elsevier: Amsterdam, 1984.
- (a) Schleyer, P. v. R.; Maerker, C.; Dransfeld, A.; Jiao, H.; Hommes, N. J. R. v. E. *J Am Chem Soc* 1996, 118, 6317; (b) Nyulaszi, L.; Schleyer, P. v. R. *J Am Chem Soc* 1999, 121, 6872; (c) Cyrański, M. K.; Krygowski, T. M.; Katritzky, A. R.; Schleyer, P. v. R. *J Org Chem* 2002, 67, 1333; (d) Patchkovskii, S.; Thiel, W. *J Mol Mod* 2000, 6, 67; (e) Schleyer, P. v. R.; Manoharan, M.; Wang, Z. X.; Kiran, B.; Jiao, H.; Puchta, R.; Hommes, N. J. R. v. E. *Org Lett* 2001, 3, 2465.
- Frisch, M. J.; Trucks, G. W.; Schlegel, H. B.; Scuseria, G. E.; Robb, M. A.; Cheeseman, J. R.; Zakrzewski, V. G.; Montgomery, J. A., Jr.; Stratmann, R. E.; Burant, J. C.; Dapprich, S.; Millam, J. M.; Daniels, A. D.; Kudin, K. N.; Strain, M. C.; Farkas, O.; Tomasi, J.; Barone, V.; Cossi, M.; Cammi, R.; Mennucci, B.; Pomelli, C.; Adamo, C.; Clifford, S.; Ochterski, J.; Petersson, G. A.; Ayala, P. Y.; Cui, Q.; Morokuma, K.; Malick, D. K.; Rabuck, A. D.; Raghavachari, K.; Foresman, J. B.; Cioslowski, J.; Ortiz, J. V.; Stefanov, B. B.; Liu, G.; Liashenko, A.; Piskorz, P.; Komaromi, I.; Gomperts, R.; Martin, R. L.; Fox, D. J.;

- Keith, T.; Al-Laham, M. A.; Peng, C. Y.; Nanayakkara, A.; Gonzalez, C.; Challacombe, M.; Gill, P. M. W.; Johnson, B.; Chen, W.; Wong, M. W.; Andres, J. L.; Gonzalez, C.; Head-Gordon, M.; Replogle, E. S.; Pople, J. A. Gaussian 98, Revision A. 11.1; Gaussian, Inc.: Pittsburgh, PA, 2001.
13. (a) For review, see Frauenheim, Th.; Seifert, G.; Elstner, M.; Hajnal, Z.; Jungnickel, G.; Porezag, D.; Suhai, S.; Scholz, R. *Phys Stat Sol* (b) 2000, 217, 41; Goringe, C. M.; Bowler, D. R.; Hernández, E. *Rep Prog Phys* 1997, 60, 1447; (b) Porezag, D.; Frauenheim, Th.; Köhler, Th.; Seifert, G.; Kaschner, R. *Phys Rev B* 1995, 51, 12947; (c) Frauenheim, Th.; Weich, F.; Köhler, Th.; Uhlmann, S.; Porezag, D.; Seifert, G. *Phys Rev B* 1995, 52, 11492; (d) Seifert, G.; Porezag, D.; Frauenheim, Th. *Int J Quantum Chem* 1996, 58, 185; (e) Elstner, M.; Porezag, D.; Jungnickel, G.; Elsner, J.; Haugk, M.; Frauenheim, Th.; Suhai, S.; Seifert, G. *Phys Rev B* 1998, 58, 7260.
14. Karni, M.; Apeloig, Y.; Kapp, J.; Schleyer, P. v. R. In *The chemistry of Organic Silicon Compounds*; Rappoport, Z.; Apeloig, Y., Eds.; John Wiley & Sons: New York, 2001; vol 3, pp 1–163.
15. (a) Li, B. X.; Cao, P. L. *J Phys Condensed Matter* 2001, 13, 10865; (b) Li, B. X.; Cao, P. L.; Zhou, X. Y. *Phys Lett A* 2001, 288, 41.
16. (a) Raghavachari, K.; Rohlfing, C. M. *J Chem Phys* 1991, 94, 3670; (b) Andreoni, W.; Pastore, G. *Phys Rev B* 1990, 41, 10243.
17. (a) Dixon, D. A.; Gole, J. L. *Chem Phys Lett* 1992, 188, 560; (b) Dai, D.; Balasubramanian, K. *J Chem Phys* 1992, 96, 8345; (c) Pacchioni, G.; Koutecky, J. *J Chem Phys* 1986, 84, 3301; (d) Andzelm, J.; Russo, N.; Salahub, D. R. *J Chem Phys* 1987, 87, 6562.
18. (a) Alford, J. M.; Laaksonen, R. T.; Smalley, R. E. *J Chem Phys* 1991, 94, 2618; (b) Zhang, Q. L.; Liu, Y.; Curl, R. F.; Tittel, F. K.; Smalley, R. E. *J Chem Phys* 1988, 88, 1670.
19. NBO Version 3.1, Glendening, E. D.; Reed, A. E.; Carpenter, J. E.; Weinhold, F.
20. Schleyer, P. v. R.; Jiao, H.; Hommes, N. J. R. v. E.; Malkin, V. G.; Malkina, O. *J Am Chem Soc* 1997, 119, 2669.
21. Bühl, M.; Hirsch, A. *Chem Rev* 2001, 101, 1153.
22. Saunders, M.; Jimenez-Vazquez, H. A.; Cross, R. J.; Mroczkowski, S.; Freedberg, D. I.; Anet, F. A. L. *Nature* 1994, 367, 256.
23. Chen, Z.; Cioslowski, J.; Rao, N.; Moncrieff, D.; Bühl, M.; Hirsch, A.; Thiel, W. *Theo Chem Acc* 2001, 106, 364.
24. Wang, C. Z.; Xu, C. H.; Chan, C. T.; Ho, K. M. *J Phys Chem* 1992, 96, 3563.